Enchained growth and cluster dislocation: A possible mechanism for microbiota homeostasis

Florence Bansept [1¤a], **Kathrin Schumann-Moor** [2¤b], **Médéric Diard** [2¤c], **Wolf-Dietrich Hardt** [2], **Emma Slack** [2¤d], **Claude Loverdo** [1] *

1 Laboratoire Jean Perrin, Sorbonne Université / CNRS, Paris, France, **2** Institute of Microbiology, Department of Biology, ETH Zürich, Switzerland

¤a Current address: Department of Evolutionary Theory, Max Planck Institute for Evolutionary Biology, Plön, Germany
¤b Current address: Center of Dental Medicine / Oral and Maxillofacial Surgery, University of Zürich, Switzerland
¤c Current address: Biozentrum, University of Basel, Switzerland
¤d Current address: Institute for Food, Nutrition and Health, Department of Health Sciences and Technology, ETH Zürich, Switzerland
* claude.loverdo@upmc.fr

Abstract

Immunoglobulin A is a class of antibodies produced by the adaptive immune system and secreted into the gut lumen to fight pathogenic bacteria. We recently demonstrated that the main physical effect of these antibodies is to enchain daughter bacteria, i.e. to cross-link bacteria into clusters as they divide, preventing them from interacting with epithelial cells, thus protecting the host. These links between bacteria may break over time. We study several models using analytical and numerical calculations. We obtain the resulting distribution of chain sizes, that we compare with experimental data. We study the rate of increase in the number of free bacteria as a function of the replication rate of bacteria. Our models show robustly that at higher replication rates, bacteria replicate before the link between daughter bacteria breaks, leading to growing cluster sizes. On the contrary at low growth rates two daughter bacteria have a high probability to break apart. Thus the gut could produce IgA against all the bacteria it has encountered, but the most affected bacteria would be the fast replicating ones, that are more likely to destabilize the microbiota. Linking the effect of the immune effectors (here the clustering) with a property directly relevant to the potential bacterial pathogeneicity (here the replication rate) could avoid to make complex decisions about which bacteria to produce effectors against.

Author summary

Inside the organism, the immune system can fight generically against any bacteria. However, the gut lumen is home to a very important microbiota, so the host has to find alternative ways to fight dangerous bacteria while sparing beneficial ones. While many studies have focused on the complex molecular and cellular pathways that trigger an immune

response, little is known about how the produced antibodies act once secreted into the intestinal lumen. We recently demonstrated that the main physical effect of these antibodies is to cross-link bacteria into clusters as they divide, preventing them from interacting with epithelial cells, thus protecting the host. These links between bacteria may break over time. Using analytical and numerical calculations, and comparing with experimental data, we studied the dynamics of these clusters. At higher replication rates, bacteria replicate before the link between daughter bacteria breaks, leading to growing cluster sizes, and conversely. Thus the gut could produce IgA against all the bacteria it has encountered, but the most affected bacteria would be the fast replicating ones, that are more likely to destabilize the microbiota. Studying the mechanisms of the immune response may uncover more such processes that enable to target properties hard to escape through evolution.

Introduction

The digestive system has a large surface area [1, 2], covered by a single layer of epithelial cells, essential for nutrient absorption, but also a gateway for many pathogens. Contrary to the inside of the body, where the presence of any bacteria is abnormal, the lumen of the digestive system is home to a very important microbiota. These microbiota bacteria are present in extremely high densities [3]. Bacteria are necessary to break down and absorb certain nutrients, and can compete against potentially pathogenic intruders [4]. Inside the organism, the immune system can fight generically against any bacteria. However, in the digestive system, the host has to find alternative ways to fight dangerous bacteria while sparing beneficial ones. As closely related bacteria (e.g. *Salmonella* spp. and commensal *E. coli*) can show highly variable behaviors in the intestine, identifying which bacteria are good or bad is challenging. Besides, the overgrowth of any type of bacteria, even those that do not cause acute pathology, can impair the functionality of the microbiota. Thus the host needs mechanisms to maintain the gut microbiota homeostasis.

The adaptive response is the only strong handle that the host has on directly controlling microbiota composition at the species level [5, 6]. The main effector of the adaptive immune response in the digestive system is secretory IgA, an antibody. sIgA specifically bind to targets that the organism has already encountered and can be elicited by vaccination. It was observed more than 40 years ago that this prevents infection by pathogenic bacteria such as *Salmonella* [7]. Many studies have focused on the complex molecular and cellular pathways that trigger an immune response on the host side of the digestive surface [8]. However, we are only just beginning to understand by which physical mechanisms the immune effectors act once secreted into the intestinal lumen, which are crucial for the control of both commensal and pathogenic bacteria. The influence on bacteria dynamics of abiotic factors such as the flow in the gut has recently started being quantitatively studied [9, 10].

We have shown that mice vaccinated with inactivated *Salmonella* Typhimurium do produce specific sIgA which bind to *S.* Typhimurium, but this neither kills them nor prevents them from reproducing [11, 12]. The initial colonization of the intestinal lumen by *S.* Typhimurium is in fact unchanged in either kinetics or magnitude in vaccinated animals. These mice are nevertheless protected against pathogen spread from the gut lumen to systemic sites like lymph nodes, liver or spleen. A classic idea in immunology is that, as one antibody has several binding sites, antibodies aggregate bacteria when they collide into each other. But this effect would be negligible at realistic densities of a given bacterium in the digestive system, simply due to very long typical encounter times between bacteria recognized by the same sIgA

(see appendix A in S1 Text). We have shown that actually, the main effect is that upon replication, daughter bacteria remain attached to one another by sIgA, driving the formation of clusters derived from a single infecting bacterium [12]. This "enchained growth" is effective at any bacterial density. Clustering has physical consequences: the produced clusters do not come physically close to the epithelial cells. And as interaction with the epithelial cells is essential for *S*. Typhimurium virulence, this is sufficient to explain the observed protective effect.

If sIgA was perfectly sticky, we would expect all bacteria to be in clusters of ever increasing size. In these experiments, despite observing *S*. Typhimurium clusters in the presence of sIgA, there are still free *S*. Typhimurium, and small clusters. One possibility would be that not all bacteria are coated with sIgA. But in these experiments, it has been demonstrated that they are (extended figure 2c of [12]). Indeed, a gram of digestive content contains at most 10^{11} bacteria, and typically 50 micrograms or more of sIgA [13], of molecular mass of about 385kD. This leads to about 800 sIgA per bacteria. sIgA may not be all bound to bacteria, and sIgA for different specific antigens may be produced in proportions not matching the proportions of antigens present in the digestive system, so that not all bacteria are coated with 800 sIgA. Nevertheless, most bacteria already encountered by the organism will be coated with many sIgA, and thus the cluster size is not limited by the number of available sIgA. Another possibility is that the sIgA-mediated links break. Such breaking has been demonstrated to be dependent on the applied forces in related systems [14, 15]. As there is shear in the digestive system, because mixing is needed for efficient nutrients absorption, it is plausible that links break over time.

Small clusters are linear chains of bacteria, bound by sIgA, with these links being broken over time by the forces induced by the flow. As bacteria are similar to each other, it is, at another scale, analogous to other physical systems [16], such as polymers breaking under flow [17]. The main difference is that these chains grow by bacterial replication. Growth and fragmentation are competing effects, and the modelling of these chains can be viewed as statistical physics, to predict their length distribution, whether there is a typical chain length, or if large chains of ever-increasing length dominate the distribution, and how the growth in number of free bacteria depends on the bacterial replication rate.

This could have very important biological consequences. To illustrate this point, let us consider a simplified model: bacteria remain enchained by sIgA when they grow (replication time τ_{div}), and this link between 2 bacteria breaks at a specific time τ_{break} (although this latter hypothesis is not realistic, we make it for now for the sake of simplicity). If $\tau_{div} > \tau_{break}$, then when a bacterium divides, it forms a 2-bacteria cluster, which dislocates into 2 free bacteria before the next replication steps, so that the bacteria remain in the state of free or 2-bacteria clusters and there are no larger clusters. If $\tau_{div} < \tau_{break}$, when a bacterium divides, it forms a 2-bacteria cluster, which becomes a 4-bacteria cluster before the first link breaks, so there cannot be free bacteria. In this model, the fast-growing bacteria are selectively targeted by the action of the immune system. The immune system does not need to sense which bacteria are growing faster, it only has to produce sIgA targeted to all the bacteria it has encountered, and bacteria with $\tau_{div} > \tau_{break}$ are unaffected, whereas bacteria with $\tau_{div} < \tau_{break}$ are trapped in clusters. That could be a simple physical mechanism to target the action of the immune system to the fast-growing bacteria which are destabilizing the microbiota, and thus to preserve microbiota homeostasis.

In the following, we present different plausible models of bacteria clusters dynamics, and the methods to study them. Then we give, for each model, the resulting dynamics and chain length distribution, before putting these results in perspective with experimental data. Eventually, we discuss the results. As some biological details are unknown, studying different models

enables to show which key results are robust; and differences confronted to experimental data give some indications about which are the most likely.

Models and methods

Ethics statement

All animal experiments were approved by the legal authorities (licenses 223/2010, 222/2013 and 193/2016; Kantonales Veterinäramt Zürich, Switzerland) and performed according to the legal and ethical requirements.

Experimental methods

We perform a new analysis on microscopy images that were produced for [12]. We analyzed images of cecal content in vaccinated mice for the early data points (4 and 5 hours) of experiments starting from a low inoculum (10^5), to minimize the clustering from random encounters. Further details on our analysis can be found in appendix G in S1 Text, as well as a brief description of the experiments from which the images were produced.

Models and general methods

We consider low bacterial densities, so encounters between unrelated bacteria are negligible. Thus, we consider each free bacteria and each cluster of bacteria independently of the others. *Salmonella* are rod-shaped bacteria, which replicate by dividing in two daughter bacteria at the middle of the longitudinal axis. Thus if the daughter bacteria remain enchained, they are linked to each other by their poles. With further bacterial replications, the cluster will then be a linear chain. This is consistent with experimental observations, in which clusters are either linear chains, with bacteria attached to one or two neighbors by their poles, or larger clusters which seem to be formed as bundles of such linear clusters (pannel A Fig 1). Our aim is to model the dynamics of these chains.

A first element is the bacterial replication (see Fig 1C). One way to model it is to assume that bacteria replicate every τ_{div}. Another way, that we will generally use, less realistic but easier for calculations, is to assume that there is a fixed replication rate r.

A second element is that when bacteria replicate, they may be able to escape enchainment (see Fig 1B), but likely with low probability (see discussion in appendix B in S1 Text). In general, we will take the limit with perfect enchainment upon replication ($\delta = \delta' = \delta'' = 0$).

A crucial element is the possibility for the links between bacteria to break. We usually assume that the breaking rate α is the same for all links and over time. We will also explore the case when the link breaking rate is force-dependent, in which case not all the links have the same breaking rate.

Another crucial element, is to model what happens when the chain breaks (see Fig 1D). If the subparts come in contact again at the same poles and get linked again, then this could simply be modeled by an effectively lower breaking rate. More likely, if the subparts come in contact again, they do so laterally, forming larger clusters of more complex shapes. Because in these clusters, most bacteria have more than two neighbors, and more contact surface, they are much less likely to escape. To simplify, we will consider that these clusters do not contribute anymore to releasing either free bacteria or linear chains. Thus when a link breaks, either the two subparts move sufficiently away and become two independent chains (probability q); or collide and become a more complex cluster which does not contribute anymore to both free bacteria and linear chains (probability $1 − q$). For simplicity, we consider that when an outermost link breaks, the single bacterium, more mobile, always escapes ($q_{outermost} = 1$), but that
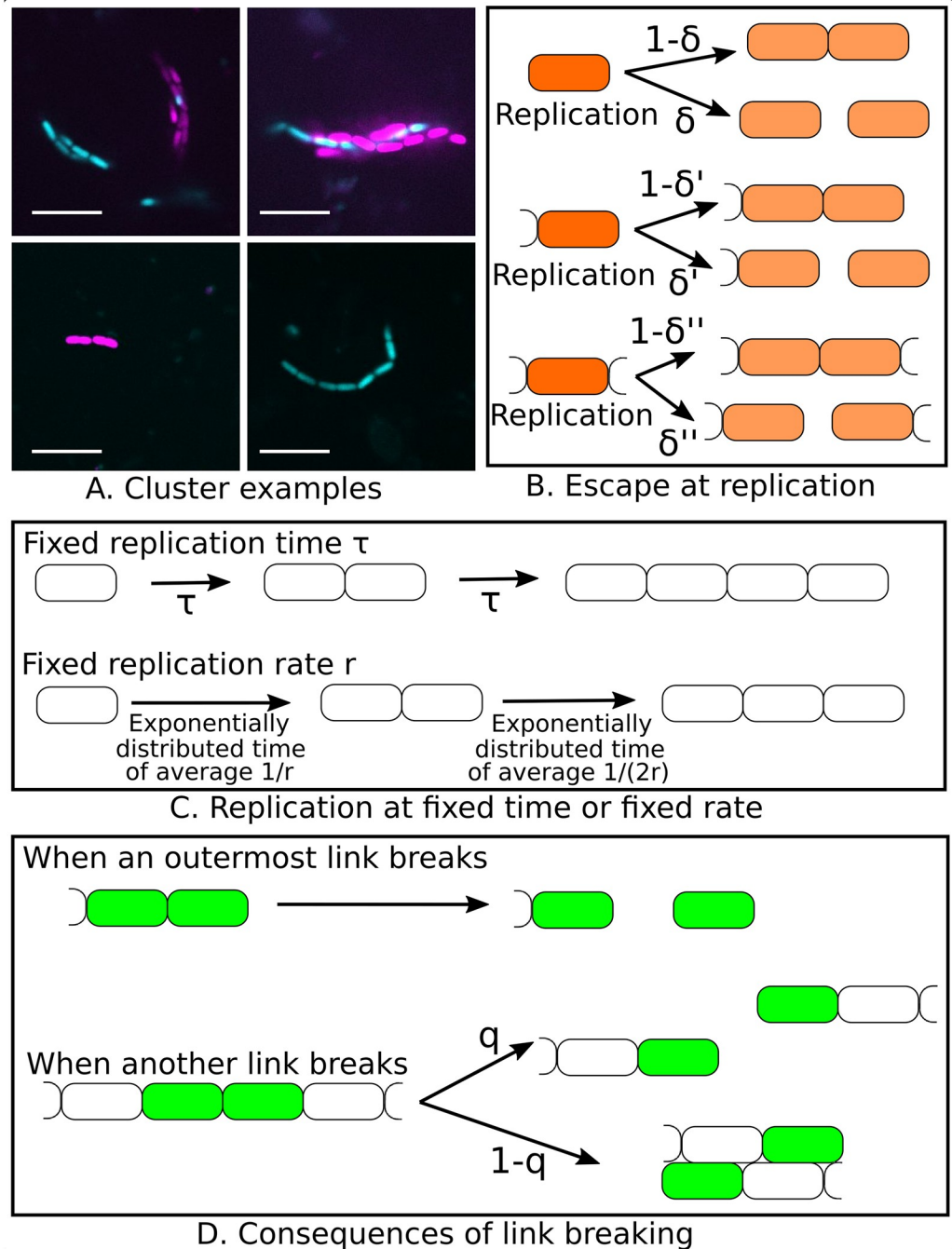
Fig 1. Bacterial cluster modeling. A. Representative experimental images of bacterial clusters in cecal content of vaccinated mouse at 5h post infection with isogenic GFP and mCherry expressing *S.* typhimurium (Experiments performed for [12]). The scale bar is $10\mu m$. Top images: complex clusters made from bundles of linear clusters, which could be re-linked single chains (left) or formed from at least two independent clones (indicated by fluorescence, right). Bottom images: linear clusters which dynamics we aim to model. B. Potential bacterial escape at replication (in the base model, $\delta = \delta' = \delta'' = 0$). C. Fixed replication time or fixed replication rate (the latter is chosen for the base model). D. Consequences of link breaking. In the base model, $q = 0$.

else q is independent of the position and the length. The simplest values to study are either $q = 0$ or $q = 1$. As we will see, when we study the case in which q can take any value between 0 and 1, we find that the case $q = 1$ is qualitatively different from other values of q. Consequently, we will take $q = 0$ for the base model.

As digestive content leaves the digestive system, or the part of the digestive system under consideration, due to flow, we define c the loss rate of free bacteria, and c' the loss rate of chains. We assume no death. Bacterial death would break chains. It would thus have a similar effect to a larger breaking rate α. As free bacteria have more autonomous motility, enabling them to swim towards the epithelial cells, it is likely that $c' \geq c$. We will usually take $c = c'$. Crucially, in this latter case, free bacteria, and all chains are lost at the same rate. The c value has a complex effect on stochastic quantities, such as the probability to have at least one chain of a given length. However, here we study the mean numbers of free bacteria and chains of different lengths, then the case with $c = c'$ is equivalent to $c = c' = 0$, with all numbers of bacteria and chains multiplied by $\exp(-ct)$.

We start with the most basic model, with a replication rate r, bacteria perfectly bound upon replication ($\delta = \delta' = \delta'' = 0$), a fixed breaking rate per link α, and bacterial chains always binding into a more complex cluster when a link breaks (except for the outermost links) ($q = 0$). We then study variations of the model to test the robustness of the results: with an non-zero escape probability upon replication and $c \neq c'$; with a replication time τ instead of a replication rate r; with the possibility for chains to escape when an inner link breaks ($q > 0$); with a force-dependent breaking rate (see Table 1 for a list of symbols).

Table 1. Recapitulation table of the symbols used.

Base model	
r	Bacterial replication rate
α	Breaking rate of the link between two bacteria
$n_i(t)$	Number of linear chains of length i at t (n_1: free bacteria)
λ	Largest eigenvalue of the matrix M, which is the growth rate of the free bacteria in the steady state
P	Eigenvector of components p_i associated to λ, normalized such as $\sum_{i=0}^{\infty} p_i = 1$.
Model with bacterial escape and bacterial loss (all these parameters are taken as 0 in the base model)	
δ	When a free bacterium replicates, the probability that this will lead to 2 free bacteria
δ'	When a bacterium at the tip of a chain replicates, the probability that the daughter bacterium at the exterior side escapes
δ''	When a bacterium replicates within a chain, the probability that the daughter bacterium will not be bond to each other, resulting to the chain breaking in two
c	Loss rate for the free bacteria
c'	Loss rate for the chains
Model with fixed replication time	
τ	Time between one bacterial division and the next (the bacterial growth rate is $r_{eff} = \log(2)/\tau$)
$\mathcal{N}$	Largest eigenvalue of the matrix in this model. $\mathcal{N} = \exp(\lambda\tau)$
Model with linear chains independent after breaking	
q	Probability that when an inner link of a chain breaks, the two subparts become independent linear chains. In the base model, $q = 0$.
Model with force-dependent breaking rate	
β	A constant expressing the strength of the coupling between hydrodynamic forces and link breaking. In the base model, $\beta = 0$.

We consider the beginning of the process, early enough so that the carrying capacity is far from reached, and thus the replication rate is constant. We do not consider generation of escape mutants which are not bound by IgA. We consider only the average numbers of free bacteria and linear chains of different lengths, and we do not count more complex clusters, as they do not contribute to free bacteria dynamics in our model. For each model, we write the equations for the derivative of these numbers with respect to time. With N the vector of the mean number of free bacteria, linear chains of length 2, 3, etc., these equations give the coefficients of the matrix M, such that $dN/dt = MN$. The results are obtained in part via analytical derivations and in part via numerical studies. The latter are obtained in Mathematica by numerically solving the eigensystem written for chains up to length n_{max}, chosen large enough not to impact the results. In the long term limit, $N(t) \to Ce^{\lambda t} P$, with C a constant, λ the largest eigenvalue of M, and P the corresponding eigenvector, normalized such that the sum of its components is equal to 1. λ is thus the long term growth rate of the free bacteria and the linear chains. For each model, we study how the growth of free bacteria—the ones which are capable of causing systemic infection [12]—which is λ in the steady state, depends on the bacterial replication rate. Besides, we obtain chain length distributions (the components p_i of P), which could be compared to experimentally observed distributions.

Results

Base model: Replication rate, no bacteria escape upon replication, fixed breaking rate, $q = 0$

Equations. In the base model, bacteria have a replication rate r, daughters are perfectly bound upon replication, each link has a breaking rate α, and when a link which is not at a tip breaks, the resulting two chains of bacteria always bind into more complex clusters and thus do not contribute to free bacteria dynamics anymore ($q = 0$). With $n_i(t)$ the number of linear chains of length i as a function of time, (n_1 is the number of free bacteria),

$$\frac{dn_1}{dt} = -rn_1 + \sum_{i=2}^{\infty} 2\alpha n_i \tag{1}$$

and for $i \geq 2$,

$$\frac{dn_i}{dt} = rn_{i-1}(i-1) - irn_i - (i-1)n_i\alpha + 2\alpha n_{i+1} \tag{2}$$

In a chain of length i, i bacteria may replicate, thus the total rate for one replication occurring in any bacterium of the chain is ir. This explains the terms $rn_{i-1}(i-1) - irn_i$. Such a chain is made of $i-1$ links, so the total breaking rate is $(i-1)\alpha$, explaining the term $-(i-1)n_i\alpha$. When the link within a chain of length two breaks (rate α per chain), two free bacteria are released. For longer chains, there are two outermost links (on each side of the chain) which breaking releases one free bacterium and one one-bacterium shorter chain. This explains the term $\sum_{i=2}^{\infty} 2\alpha n_i$ in Eq (1) and the term $2\alpha n_{i+1}$ in Eq (2).

Free bacteria growth rate as a function of the bacterial replication rate. Even for this simple version, the system of equations is hard to solve in the general case. We start by studying numerically the growth rate in the long term (the maximum eigenvalue λ of the matrix of coefficients $m_{i,j} = r(i-1)\delta_{i-1,j} - ir\delta_{i,j} - (i-1)\alpha\delta_{i,j} + 2\alpha(\delta_{i+1,j} + \delta_{i,1}(1 - \delta_{j,1} - \delta_{j,2}))$, with $\delta_{i,j}$ the Kronecker symbol, which takes the value 1 when $i = j$, and 0 otherwise), as a function of the replication rate (see Fig 2A). The growth rate has a maximum for a finite replication rate, of the order of α (the link breaking rate): the higher the replication rate, the higher the potential
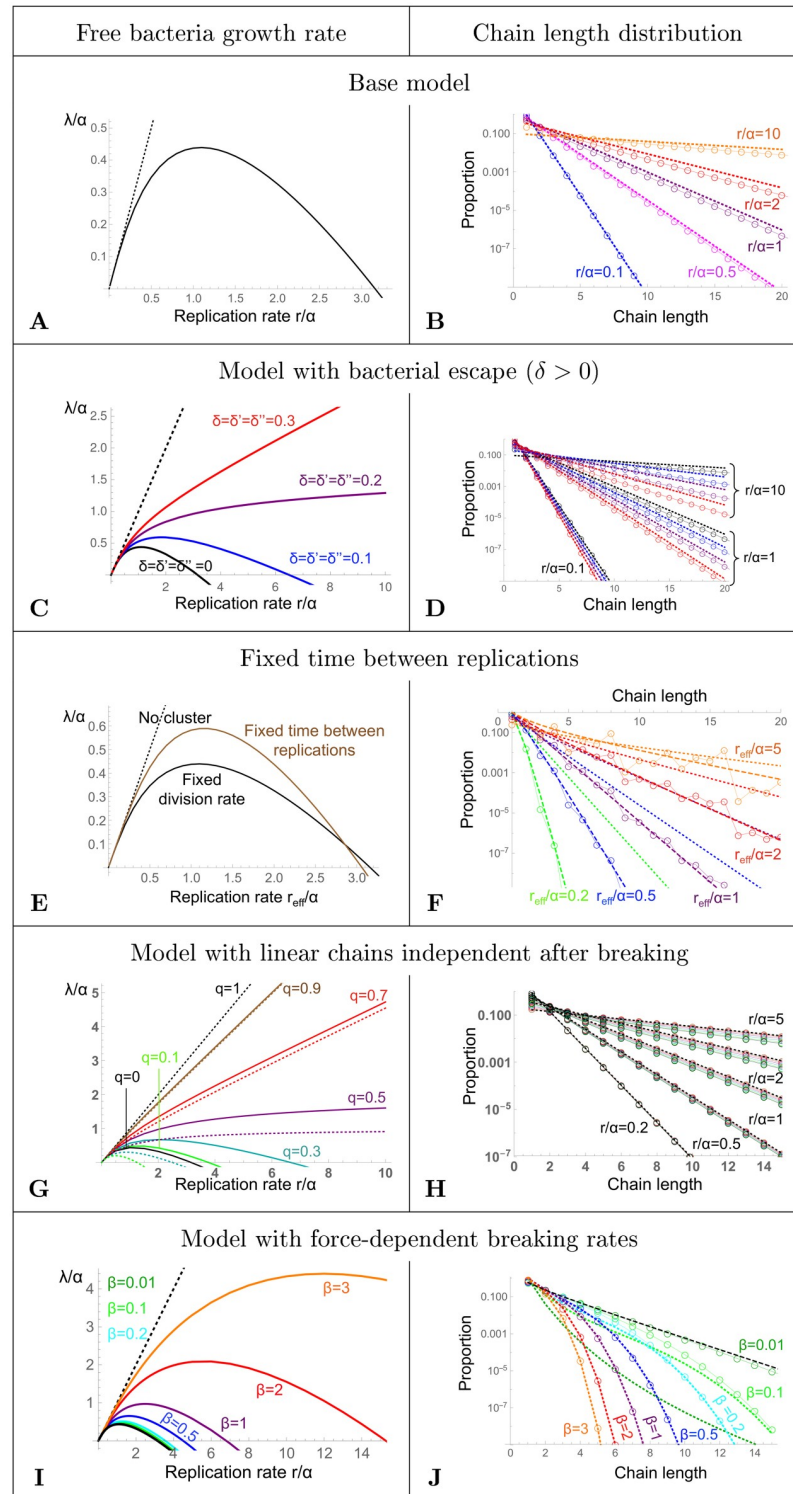
Fig 2. Left panels A, C, E, G, I: Growth rate λ of the free bacteria as a function of the bacteria replication rate r, both in units of α. Numerical results (solid colored lines), and limit with no clusters ($\lambda = r$) (black dotted line). The base model is represented in black in all the left panels to ease comparison between models. **Right panels B, D, F, H, J**: Chain length distribution. Open circles linked by solid lines: numerical results. **A, B: Base model**, $n_{max} = 40$. B. dotted lines: approximation (5) (almost overlaid with the numerical results for $r/\alpha = 0.1$). **C, D: Model with bacterial escape**. $\delta = \delta' = \delta'' = 0$ (green), 0.1 (blue), 0.2 (purple), 0.3 (red). $c = c' = 0$, $n_{max} = 40$. D. dotted lines: approximation (9). **E, F:**

Fixed time between replications. $r_{eff} = \log(2)/\tau$. $n_{max} = 32$. F. approximation (18) (dashed lines), numerical result in the base model (dotted lines). $r_{eff}/\alpha = 0.2$ (green), 0.5 (blue), 1 (purple), 2 (red), 5 (orange). **G, H: Model with linear chains independent after breaking**. G. The dotted black line is the case $q = 1$, for which $\lambda = r$, like in the absence of clusters. The colored dotted lines are the analytical approximation (28). $n_{max} = 200$. H. The dotted black lines are the approximate distribution (26) for each r/α, which is the exact distribution for $q = 1$. The colours represent the same q values than for the left panel. All curves are almost overlaid for small r. $n_{max} = 80$. **I,J: Model with force-dependent breaking rates**. Each color represents a different β. Darker green: $\beta = 0.01$ ($n_{max} = 20$); green: $\beta = 0.1$ ($n_{max} = 15$); cyan: $\beta = 0.2$ ($n_{max} = 15$); blue: $\beta = 0.5$ ($n_{max} = 15$); purple: $\beta = 1$ ($n_{max} = 15$); red: $\beta = 2$ ($n_{max} = 10$); orange: $\beta = 3$ ($n_{max} = 10$). I. The black line is the numerical result for the base model, equivalent to $\beta = 0$. The curve for $\beta = 0.01$ (dark green) is almost overlaid with the curve for $\beta = 0$. J. Chain length distribution for $r/\alpha = 1$. The colored dotted lines the analytical approximation (32), and the black dashed line the numerical result for the base model.

for growth in the number of free bacteria, but when the replication rate becomes too large compared to the breaking rate, the bacteria get trapped in clusters, which break and re-attach in more complex clusters from which independent bacteria cannot escape.

Chain length distribution. In the long time limit, the number of chains of length i is of the order of $Cp_i \exp(\lambda t)$, with λ the largest eigenvalue. Eq (2) simplifies to:

$$\lambda p_i = -ir p_i + r p_{i-1}(i-1) - (i-1)p_i \alpha + 2\alpha p_{i+1} \tag{3}$$

Assuming that i is large,

$$p_i \simeq \frac{r}{r + \alpha} p_{i-1} \tag{4}$$

is required. Using this approximation for all i, the proportion of chains of length k among linear chains and free bacteria is:

$$p_k = \left(1 - \frac{r}{r + \alpha}\right)\left(\frac{r}{r + \alpha}\right)^{k-1} \tag{5}$$

This approximation works relatively well, especially for smaller r/α values (see Fig 2B). Part of the discrepancy is that Eq (4) is an approximation for large i, and thus does not hold at small chain length.

Model with bacteria escape

Equations. This is similar to the base model presented before, except that we take into account that upon replication, bacteria may not be perfectly bound, and may escape (Fig 1B). We denote δ the probability for the two daughter bacteria to become free bacteria upon replication of a free bacterium. We denote δ' the probability that when a bacteria at the tip of a chain replicates, the daughter bacterium on the outside of the chain escapes the enchainment. We denote δ'' the probability that when a bacterium at the interior of the chain divides, the daughter bacteria will not be enchained, effectively clipping the chain in two. As free bacteria are more motile than clusters, then $\delta \geq \delta' \geq \delta''$. We also add here the possibility that the loss rate c for free bacteria and c' for chains are different. Then the base equations are:

$$\frac{dn_1}{dt} = r(-1 + 2\delta)n_1 + \sum_{i=2}^{\infty} 2r\delta' n_i + \sum_{i=2}^{\infty} 2\alpha n_i - cn_1 \tag{6}$$

$$\frac{dn_2}{dt} = r(1 - \delta)n_1 - 2r(1 - \delta')n_2 - \alpha n_2 + 2n_3\alpha - c'n_2 \tag{7}$$

and for $i \geq 3$,

$$\frac{dn_i}{dt} = r(2\delta' - i)n_i + rn_{i-1}(i - 1 - 2\delta' + 3\delta'' - i\delta'') - (i - 1)n_i\alpha + 2\alpha n_{i+1} - c'n_i. \quad (8)$$

Free bacteria growth rate as a function of the bacterial replication rate. Similarly to the base model, we study numerically the growth rate as a function of the replication rate (Fig 2C). The larger the replication rate, the more the deviation between the growth rate and the replication rate, which would be its value in the absence of clusters. If $\delta, \delta', \delta''$ are small enough, the qualitative behavior is similar to the base model. But for larger δ, δ' and δ'', the growth rate continues to increase monotonically with the replication rate. The same is true when δ, δ' and δ'' are different (see Fig A in S1 Text). If $c = c'$, the growth rate is simply offset by minus the loss rate (see Fig A in S1 Text), and if $c \neq c'$, the effect is more complex, but for small r/α values it corresponds to an offset of $-c$.

Chain length distribution. We can reason similarly to the base model (more details in appendix C in S1 Text), and find:

$$p_k = \left(1 - (1 - \delta'')\frac{r}{r + \alpha}\right)\left((1 - \delta'')\frac{r}{r + \alpha}\right)^{k-1} \quad (9)$$

This approximation works relatively well (Fig 2D, and Fig B in S1 Text). The approximation (9) depends on δ'', but neither on δ nor δ', but δ and δ' could actually matter when i is small, and indeed we observe (see Fig C and D in S1 Text) that the approximation (9) works slightly less well when δ'' is different from δ or δ'. If $c = c'$, the distribution is exactly the same as for $c = c' = 0$, and if $c \neq c'$, the distribution changes very little (Fig E in S1 Text).

Model with fixed replication time

In this variant of the base model, bacteria divide every τ. The effective growth rate is r_{eff} such that $\exp(r_{eff} t) = 2^{t/\tau}$, thus $r_{eff} = \log(2)/\tau$.

Equations. Let us start by considering a chain of n bacteria at $t = 0$, right after a replication event. Let us denote $l(n, i, t)$ the probability that at t, this chain has lost i bacteria in total on the extremities, and consequently is of length $n - i$ at t ($n \geq 2$ and $0 \leq i \leq n - 2$). Before the next replication event, since we assume $q = 0$ as in the base model (meaning that if the chain breaks somewhere else, the subparts form a more complex cluster and thus are "lost" for the system), we have:

$$\frac{dl(n, i, t)}{dt} = -\alpha(n - 1 - i)l(n, i, t) + 2\alpha l(n, i - 1, t). \quad (10)$$

At $t = 0$, $l(n, 0, 0) = 1$ and for $0 < i < n - 1$, $l(n, i, 0) = 0$. It can be checked easily that the following expression is the solution of (10), with $l(n, 0, 0) = 1$ and $l(n, i > 0, 0) = 0$, for any $0 \leq i \leq n - 2$:

$$l(n, i, t) = \frac{2^i}{i!}\exp(-\alpha t(n - 1))(\exp(\alpha t) - 1)^i. \quad (11)$$

Any chain of length > 2, has two outermost links, each breaking at rate α, liberating one free bacterium. A chain of length 2 breaks at rate α, but liberates two free bacteria. Starting from a unique chain of length n, the probability that a linear chain of length $n - i$ is present at time t is $l(n, i, t)$. Consequently, the total rate of production of free bacteria at time t is $2\alpha \sum_{i=0}^{n-2} l(n, i, t)$.

Thus, the average number of free bacteria generated during τ by this chain of n bacteria is:

$$\aleph_{free}(n,\tau) = 2\alpha \sum_{i=0}^{n-2} \int_0^\tau l(n,i,t)dt = 2\alpha \sum_{i=0}^{n-2} \int_0^\tau \frac{2^i}{i!} \exp(-\alpha t(n-1))(\exp(\alpha t) - 1)^i dt. \quad (12)$$

A chain of length n right before replication becomes a chain of length $2n$ upon it, and will have contributed to chains of length k by $l(2n, 2n-k, \tau)$, and to free bacteria by $\aleph_{free}(2n, \tau)$ right before the next replication event. With $n_i(t)$ the number of chains of length i at time t (right before a replication event), we can write the matricial relation between the $n_i(t)$ and $n_i(t + \tau)$ (right before the next replication event) as follows:

$$\begin{pmatrix} n_1(t+\tau) \\ n_2(t+\tau) \\ n_3(t+\tau) \\ n_4(t+\tau) \\ \vdots \end{pmatrix} = \begin{pmatrix} \aleph_{free}(2,\tau) & \aleph_{free}(4,\tau) & \aleph_{free}(6,\tau) & \dots & \dots \\ l(2,0,\tau) & l(4,2,\tau) & l(6,4,\tau) & \dots & \dots \\ 0 & l(4,1,\tau) & l(6,3,\tau) & \dots & \dots \\ 0 & l(4,0,\tau) & l(6,2,\tau) & \dots & \dots \\ 0 & 0 & l(6,1,\tau) & \dots & \dots \\ 0 & 0 & \vdots & \ddots & \ddots \end{pmatrix} \begin{pmatrix} n_1(t) \\ n_2(t) \\ n_3(t) \\ \vdots \\ \vdots \end{pmatrix} \quad (13)$$

This matrix is then cut to size $n_{max} \times n_{max}$, and the corresponding eigensystem is solved numerically.

Free bacteria growth rate as a function of the bacterial replication rate. The shape of the relation between free bacteria growth rate and (effective) replication rate (Fig 2E) is very similar in the fixed replication time vs. fixed replication rate models, with a maximum of the growth rate for a finite value of the (effective) replication rate, at close values ($r_{eff} = 1.15\alpha$ vs. $r = 1.09\alpha$). When the replication is at fixed time intervals instead of a fixed replication rate, the maximum growth rate is higher, and it dips faster at increasing effective replication rate. Indeed, in the case of fixed replication rate, the distribution of durations between two replications is exponential, thus more spread. Close to the maximum, the presence of short replication intervals makes that there can be more cluster formation, and conversely, at higher replication rates, the presence of longer replication intervals results in more production of free bacteria.

Chain length distribution. We show here the main steps to calculate analytically an approximation for the chain length distribution, and more details are given in appendix D in S1 Text. We define $n_i(t)$ the number of chains of length i at t with t taken just before a replication. Assuming i even,

$$n_i(t+\tau) = \sum_{j=0}^{\infty} n_{i/2+j}(t)l(i+2j, 2j, \tau). \quad (14)$$

In the long time limit, $n_i(t) = Cp_i \exp(\lambda t)$, with λ the long term growth rate, that is such that $\exp(\lambda\tau) = \mathcal{N}$, with $\mathcal{N}$ the largest eigenvalue of the matrix of Eq 13. Then previous equation leads to:

$$\mathcal{N}p_i = \sum_{j=0}^{\infty} p_{\frac{i}{2}+j} e^{-\alpha\tau(i-1+2j)} (e^{\alpha\tau} - 1)^{2j} \frac{2^{2j}}{(2j)!}. \quad (15)$$

We make the assumption that the first term of the sum is large compared to the rest of the sum

(assumption discussed in appendix D in S1 Text). Then,

$$p_i \simeq \frac{1}{\mathcal{N}} p_{\frac{i}{2}} e^{-\alpha\tau(i-1)}$$ (16)

and recursively, for $i = 2^k$, with k integer,

$$p_i \simeq p_1 i^{\frac{\alpha\tau - \log(\mathcal{N})}{\log(2)}} e^{-2\alpha\tau i}.$$ (17)

When $\alpha\tau \gg 1$, links typically break before the next replication, thus there is little impact of the clustering on the growth. Consequently, the growth will be close to its value in the absence of clustering, i.e. doubling every τ, and thus in this limit $\mathcal{N} = 2$:

$$p_i \simeq p_1 i^{\frac{\alpha\tau}{\log(2)} - 1} e^{-2\alpha\tau i} = p_1 i^{\frac{\gamma}{r_{eff}} - 1} 2^{-2i\alpha/r_{eff}}.$$ (18)

This rough approximation allows to explain the core of the observed distribution (Fig 2F). There are bumps, due to the replication every τ (which in the absence of link breaking would results in chains of length 2^k only), which makes that chains of power-of-two length are over-represented. Compared to the case with fixed replication rate, the distribution is much narrower (Fig 3).

Model with linear chains independent after breaking ($q > 0$)

Limit case: Subchains always remain independent linear chains after breaking ($q = 1$). In this model, when a chain breaks, the two resulting chains remain independent and can thus continue to participate in the dynamics of the system:

$$\frac{dn_i}{dt}(t) = (i-1)r\, n_{i-1}(t) + (-\alpha(i-1) - ir)\, n_i(t) + 2\alpha \sum_{j=i+1}^{\infty} n_j(t)$$ (19)

We recognize here the equation studied in [18], where they described chains of growing unicellular algae. As it has been shown, the steady state solution of the system is:

$$n_i(t) = C \exp(rt) \left(\frac{r}{\alpha + r}\right)^i,$$ (20)

with C a constant dependent on the initial state of the system. In the steady state, the growth rate is equal to the replication rate. Note that the resulting chain length distribution is then
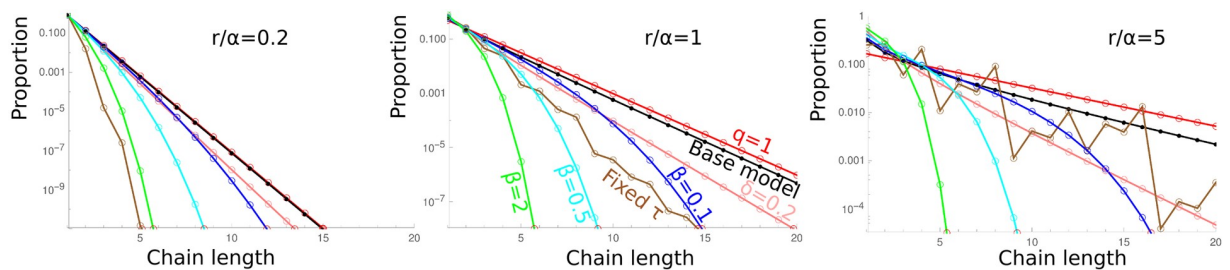

Fig 3. Comparison of the chain length distributions for the different models. The base model is represented in black. For the case with bacterial escape when a bacterium replicates, one numerical value is represented ($\delta = \delta' = \delta''$) (pink), the lower this value, the closer to the base model. The model with fixed replication time is represented in brown (for this model we choose $\tau = log(2)/r$). The model with linear chains independent after breaking ($q > 0$) is shown in red for $q = 1$, the most different from the base model. All intermediate q values are between the black and the red curves. The model with the force dependent breaking rate is represented for 3 values of β: 0.1 (blue), 0.5 (cyan), 2 (green). All the results are numerical, using n_{max} values as in Fig 2, except for $q = 1$ which is an exact analytical result.

https://doi.org/10.1371/journal.pcbi.1006986.g003

exactly equal to its approximation in the base model (5). The average chain length is $1 + \frac{r}{\alpha}$, which shows that, as expected, if the link breaking rate is high compared to the replication rate ($r/\alpha \ll 1$), the average length is close to one as no cluster has the time to form: all the bacteria remain free.

Intermediate case: Chains can either be independent or trapped after breaking. More realistically, after breaking, chains will have some probability to either encounter each other and remain trapped in more complex clusters, or to escape and become independent. We will assume in the following that if a chain of length N breaks at a link at the extremity, releasing a chain of length $N - 1$ and a free bacterium, then the free bacterium, smaller and likely more mobile, will escape in all cases; but that if the link that breaks is elsewhere, the probability for the new chains of lengths $N - k$ and k ($k > 1$) to escape and continue as two independent linear chains will be q, and the probability that they bind and form a more complex cluster will be $1 - q$, with q independent of k. We write the equations for the number $n_i(t)$ of chain of i bacteria:

$$\frac{dn_1}{dt} = -rn_1 + 2\alpha \sum_{j=2}^{\infty} n_j \tag{21}$$

$$\frac{dn_i}{dt} = -rin_i + r(i - 1)n_{i-1} - \alpha(i - 1)n_i + 2\alpha n_{i+1} + 2\alpha q \sum_{j=2}^{\infty} n_{i+j}. \tag{22}$$

In the long time, $n_i(t) \to Cp_i \exp(\lambda t)$ with λ the largest eigenvalue.

$$\lambda p_i = -rip_i + r(i - 1)p_{i-1} - \alpha(i - 1)p_i + 2\alpha p_{i+1} + \sum_{j=i+2}^{\infty} 2\alpha q p_j \tag{23}$$

This is valid for any i. We assume that p_i decreases fast enough with i such that the sum from $i + 2$ to ∞ of the p_i is an order of magnitude less than ip_i. Then, the largest elements of Eq (23) when i is large enough are the terms multiplied by i, and consequently:

$$0 \simeq -rp_i + rp_{i-1} - \alpha p_i \tag{24}$$

Leading to:

$$p_i \simeq \frac{r}{\alpha + r} p_{i-1} \tag{25}$$

If this is valid for any i, the proportion of chains of length k among linear chains and free bacteria is:

$$p_k = \frac{\alpha}{\alpha + r} \left(\frac{r}{\alpha + r} \right)^{k-1}. \tag{26}$$

Note that this expression does not depend on q and is the same as the approximation for the base model (5) and the exact expression for $q = 1$. We compare this approximation with the numerical results and they are in good agreement (Fig 2H), except when both q is small and r/α is large, and even in this case it gives a reasonable approximation.

Replacing p_i by its expression (26), Eq (23) simplifies to:

$$\lambda \simeq -r\left(1 + \frac{\alpha}{r}\right) + \alpha + 2\alpha \left(\frac{r}{\alpha + r}\right) + \sum_{j=2}^{\infty} 2\alpha q \left(\frac{r}{\alpha + r}\right)^{j} \tag{27}$$

which after simplifications leads to:

$$\lambda \simeq r \frac{\alpha + (2q - 1)r}{\alpha + r}. \tag{28}$$

This approximation does not work for $q < 0.5$, but it works well for q close to 1, and gives the right slope for r/α large for $q > 0.5$ (Fig 2G). We can observe that for $q > 0.5$, λ increases indefinitely when r increases; but it has an intermediate maximum for $q < 0.5$. Intuitively, if $q > 0.5$, when a chain breaks it leads to more than one independent linear chain, thus the population of linear chains (and, consequently, of free bacteria as well) may increase monotonically with r/α. On the contrary, if $q < 0.5$, chains that break lead to less than one independent chain on average, and thus the behaviour of the system is more determined by the fate of the chains, and thus closer to the results for $q = 0$, for which the growth rate λ has a maximum as a function of r.

The proportion of free bacteria relative to the total number of bacteria is proportional to $\exp(\lambda t)/\exp(rt)$, which, using approximation (28) tends to $\exp(-2r^2 t(1 - q)/(r + \alpha))$. The proportion of free bacteria thus decreases over time, and decreases with increasing replication rate r. Thus the proportion of bacteria trapped in clusters, which is 1 minus the proportion of free bacteria, increases with increasing replication rate even when $q > 0.5$.

Model with force-dependent breaking rate

Equations. What drives link breakage? The links could break if there was some process degrading the sIgA, but the sIgA are thought to be very stable [19]. Another possible explanation for link breaking is that the bound antigen can be extracted from the bacterial membrane, at a rate which may vary exponentially with the force [15, 20]. The forces applied on the links are likely mostly due to the hydrodynamic forces exerted by the digesta flow on the bacterial chain. Taking the linear chain as a string of beads, as done for polymer chains, and in a flow with a constant shear rate, the force is predicted to be larger as the chain grows longer, and the largest at the center of the chain [17]. A more detailed discussion and the calculations can be found in appendix E.1 in S1 Text. Taking α as the breaking rate in the absence of shear, and β a constant expressing the strength of the coupling between hydrodynamic forces and link breaking, the resulting equations for this minimal model taking into account the forces are:

$$\frac{dn_1}{dt} = -rn_1 + 2 \sum_{i=2}^{\infty} \alpha n_i \exp\left(\beta \frac{i - 1}{2} \right) \tag{29}$$

and for i even,

$$\frac{dn_i}{dt} = -rin_i - \alpha n_i e^{\beta i^2/8} \left(1 + 2 \sum_{j=2}^{i/2} e^{-(j-1)^2 \beta/2} \right) + r(i - 1)n_{i-1} + 2\alpha n_{i+1} e^{\beta i/2} \tag{30}$$

and for $i > 1$ odd,

$$\frac{dn_i}{dt} = -rin_i - 2\alpha n_i e^{\beta i^2/8} \sum_{j=1}^{(i-1)/2} e^{-(j-1/2)^2 \beta/2} + r(i - 1)n_{i-1} + 2\alpha n_{i+1} e^{\beta i/2} \tag{31}$$

Free bacteria growth rate as a function of the bacterial replication rate. The growth rate as a function of the replication rate has a qualitatively similar shape as for the base model (Fig 2I), with a finite replication rate maximizing the growth rate. The limit $\beta \to 0$ corresponds

well to the base model, as expected. When β increases, the replication rate maximizing the growth rate increases, as the effective breaking rate is higher. Numerically, we find (see Fig G in S1 Text) that the replication rate maximizing the growth rate scales as $\alpha \exp(0.8\beta)$.

Chain length distribution. Similarly to the other models, for t long enough, $n_i \simeq C p_i \exp(\lambda t)$ (with λ the largest eigenvalue), and assessing which terms in Eqs (30) and (31) will be dominant, we ultimately obtain (details in supplementary section 5.3):

$$p_i \simeq \left(\frac{r}{\alpha}\right)^{i-1} \frac{(i-1)!}{Y^{floor(i/2)} Z^{floor((i-1)/2)}} \exp\left(-\frac{\beta}{8}\left(-1 + \frac{i + 3i^2 + 2i^3}{6}\right)\right), \qquad (32)$$

with $Y = 1 + 2\sum_{j=1}^{\infty} \exp(-\beta j^2/2)$ and $Z = 2\sum_{j=1}^{\infty} \exp(-\beta(j-1/2)^2/2)$. This approximation works well, except for small β (Fig 2J, and Fig H in S1 Text). Compared to the base model, the number of chains decreases much faster with their length (See Figs 2J and 3). Indeed, the breaking rates for each link increase importantly with the chain length, thus larger chains are much less stable than in the base model.

Comparison with experimental data

We analyzed (see appendix G in S1 Text) microscopy images of cecal content from vaccinated mice infected with *S.* Typhimurium, which were acquired for our previous study [12]. Most clusters are large, and of complex shape. But smaller clusters are linear, and we obtained the distribution shown by the black line and points in Fig 4. The model with fixed division time is *a priori* more realistic. The best fit is obtained with this model, with the one
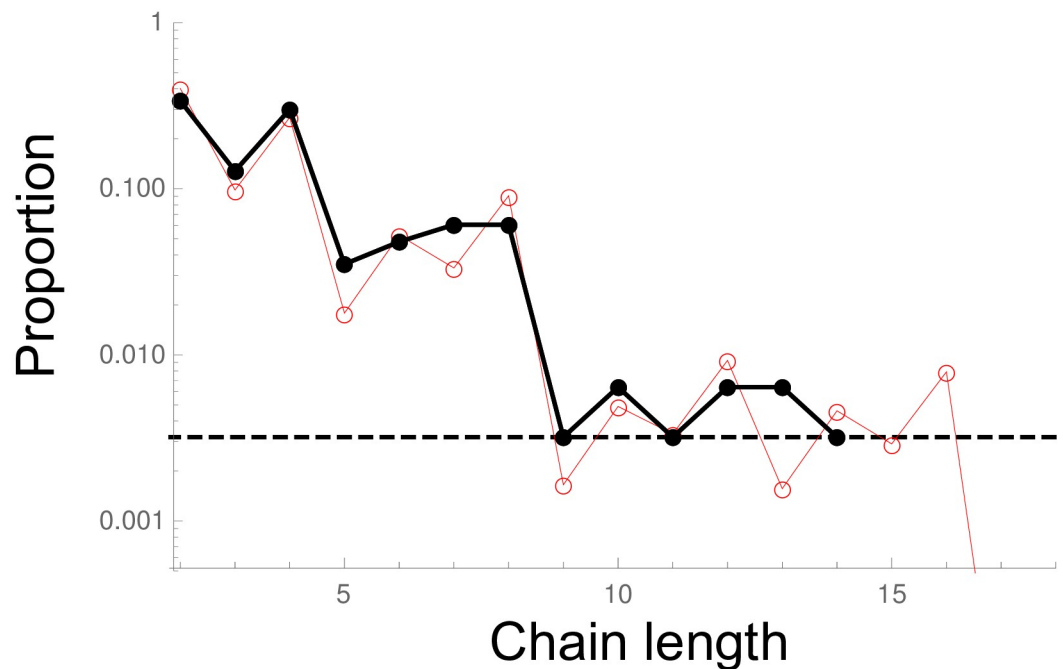

Fig 4. Comparison with experiments. Chain length distribution (proportions relative to the linear chains of length ≥ 2 are represented in log scale). The black dots and line are the experimental data. The horizontal dotted black line represents the case in which there is one chain of the given size. No chains longer than size 14 were detected in our experimental images. The red line and points are the numerical results for the model with fixed replication time. In this model, there is only one free parameter, $r_{eff}/\alpha = \log(2)/(\alpha\tau)$, which fitted value is 4.1 (see appendix G in S1 Text for more details).

adjustable parameter $r_{eff}/\alpha = 4.1$ (red line and points) with estimated 95% confidence interval $[3.6 - 4.7]$. It seems however, though there is not enough data to quantitatively ensure it, that there are less long clusters than expected (see appendix G.3 in S1 Text for an expanded discussion). The data may be biased, as longer chains may not be fully in the focal plane. That the distribution is relatively narrow could also be compatible with force-dependent breaking rates.

Discussion

We started from the recent finding [12] that the protection effect of sIgA, the main effector of the adaptive immune system in the gut, can be explained by enchained growth. Because sIgA are multivalent, they can stick identical bacteria together if they encounter each other. Early in infection, bacteria of the same type are at low density, thus typical encounter times are very long, but when a bacterium replicates, the daughter bacteria are in contact and thus can remain enchained to each other by IgA. Bacteria in clusters are less motile than individual bacteria, and in particular, are not observed close to the epithelial cells. In the case of wild type *S.* Typhimurium, only free bacteria which can interact with the epithelial cells contribute to the next steps of the infection process. Despite the presence of sIgA, some free bacteria are observed. It could be that they escape at the moment of replication. But, along with the observation that clusters do not grow indefinitely, it could also be a sign that the links between bacteria break. It is also physically expected that the links have some finite breaking rate. If the typical time between two bacterial divisions is much larger than the typical time for the link to break, then there would be no cluster. Conversely, in the inverse case, bacteria will be very likely to be trapped in large clusters. Then, even if sIgA are produced against all bacterial types, the bacteria dividing faster will be disproportionately affected.

We investigated if this qualitative idea holds with more realistic models. We started from a base model in which: bacteria replicate at a fixed rate; remain enchained upon replication; until the link between them breaks at a given fixed breaking rate, identical for all links; and considering that, because of the way bacteria such as *Salmonella* or *E.coli* divide, the early clusters are linear chains of bacteria; when the chain breaks at an outermost link, we assumed the free bacteria will escape; but if the chain breaks elsewhere, we assumed that the two resulting sub-chains encounter each other quickly and form clusters of more complex shapes from which individual bacteria do not escape. We studied this base model with a combination of analytical and numerical approaches. We also tested the robustness of our findings by studying separately several variations of the base model: a probability of escaping upon replication, loss rates, fixed replication time, non-zero probability for the subchains to escape, and force-dependent breaking-rates. For each model, we studied how the growth rate of the free bacteria varies with the replication rate (which would be equal if there were no clusters), and the distribution of chain lengths.

We find that, except in the very specific case in which subchains always escape upon link-breaking ($q = 1$), the growth rate of the number of free bacteria is lower than the replication rate. And more spectacularly, in most of the models studied (but not if more than half the sub-chains escape upon link breaking, or if there is a significant probability for bacteria to escape enchainement upon replication), the growth rate of the number of free bacteria is non-monotonic with the replication rate: there is a finite replication rate which maximizes the growth rate of non-clustered bacteria. At very high replication rates, bacteria get trapped in more complex clusters and cannot contribute anymore to the free bacteria dynamics and thus to the next steps of the infection process. The replication rate maximizing the growth rate is of the order

of the breaking rate, though its specific value depends on the details of the model. To summarize, except when $q = 1$, we always find that the higher the replication rate, the higher the proportion of bacteria trapped into clusters; and in many cases, the effect is even more dramatic, with the growth rate of free bacteria that may decrease with the replication rate.

The chain length distribution depends on the model (see Fig 3). In most cases, the proportion of linear chains having length k decreases as γ^k, with γ some constant smaller than 1. When replication occurs at fixed time, or when breaking rates are force-dependent, the proportion of longer chains decreases faster. There are models with different chain length distributions but qualitatively similar dependence of the growth rate on the replication rate, and the opposite is true too. This shows that large clusters have little importance for free bacteria production, what matters most is the small chains dynamics. It is reassuring, as we did not consider buckling, which would make long linear chains fold on themselves and produce more complex clusters, and may bias the linear chain distribution for very large lengths. It should also be noted that with fixed division time, not only the distribution is bumpy, as chains comprising a power of two number of bacteria are more frequent than others, but the distribution is also narrower.

We analyzed experimental data on clusters of *S.* Typhimurium in the cecum of vaccinated mice. The experimental chain length distribution is in line with the model of fixed replication time, which is indeed more realistic. There is however somewhat less large chains than expected. More data would be necessary to asses this more reliably. This could be because of possible bias in the data. This could be also compatible with force-dependent breaking rates. Additional experiments, for instance to measure the breaking rate, could help by giving additional independent information and constrain the fitting. To test the dependence of the growth rate with the replication rate, an ideal experiment would be to compare similar bacterial strains, but with differing replication rates, and compete them in the same individual. It is however very challenging to obtain bacteria that differ only by their replication rate, particularly in vivo.

sIgA-enchained bacterial clusters could be studied in vitro to measure how they break. However, using in vitro results to draw conclusions on in vivo systems is limited. First, there could be chemical or enzymatic components of the lumen that could facilitate or hinder link breaking, and the non-Newtonian viscosity of the digesta could play a role in the mechanic forces felt by the links, thus a simple buffer may not mimic well the real conditions. More crucially, the exact forces felt by particles of the size of bacterial clusters are not well characterized. Most studies of the flow characteristics in the digestive system rely either on external observations of the peristaltic muscles [21] or indirect measures of times for a marker to exit some section of the digestive track [22]. More quantitative study of the digestive flow at small scales is just beginning [9, 10, 23–27] and in the future it may give more clues to assess to which forces bacteria are subjected to in the digestive track.

The mechanism we propose is nevertheless plausible. The observation in vaccinated mice of the existence of single bacteria and small clusters, and particularly small linear chains with an odd number of bacteria, are pieces of evidence that clusters do break in these in vivo conditions. An alternative explanation could be that some bacteria escape enchainement upon replication. However, at higher bacterial densities, we have evidence of independent bacteria binding when they encounter [12], thus sIgA coated bacteria are adhesive. When two daughter bacteria divide, they are in contact, thus if sIgA is adhesive, escape is unlikely (see appendix B in S1 Text). Importantly, even though our results show that specific conditions are needed for the growth rate to decrease with high replication rates, we almost always find that the higher the replication rate, the higher the proportion of bacteria trapped in clusters. Thus, even when it does not reverse the relationship between the growth rate of the free bacteria and the

replication rate, it is at least dampening this relationship, and can be a tool both to control pathogenic bacteria, but also to maintain homeostasis of the gut microbiota. It is also interesting that there are other host effectors besides sIgA that bind bacteria together: neutrophil extracellular traps for instance [28], and there could also be an interplay between replication rates and the breaking of the links mediated by these other effectors, as the mechanism we propose here is generic.

As for any mechanism to fight against bacteria, the question of how easily resistance can be evolved is crucial. On the one hand, the replication rate could evolve. But bacteria replicating slower would be less competitive with other bacteria in the absence of sIgA, and a slower growth leaves more time for further host response. On the other hand the typical link breaking time could evolve. On the host side, sIgA is thought to be mechanically very stable, and experiments about the bonding of cells by sIgA seem to point to the link failing because of the extraction of the antigen rather than because of sIgA breaking, and rather than the sIgA/antigen bond detaching [14, 20]. In the case of IgA defficiency, there is more secretion of IgM, and microbiota is disturbed [29]: we may speculate that IgM being less powerful for microbiota homeostasis is related to these immunoglobulins being more protease-sensitive than IgA and thus cleaved on shorter time scales [30]. On the other side, bacteria could evolve surface antigens. It could be interesting to think that bacteria could produce decoy antigens with no functional value, but against which the immune system will mount an immune response, and that are more easily released from the bacteria, thus disabling the main sIgA mode of action (being easily evolvable would also be a benefit). Such decoys would however be a metabolic cost for the bacteria, and when breaking, may unmask other antigens corresponding to crucial functions of the bacteria. It could be argued that the capsule around bacteria such as *Salmonella* spp., and also common in pathogenic *E.coli*, may behave as a decoy, though it has also other functions. Evolving resistance to IgA-mediated enchainment would thus be costly.

Along the same lines, we may speculate whether mechanical aspects could be a reason why sIgA against some antigens are not efficient for protection. For instance, while anti-flagella sIgA aggregate very well *Salmonella* Enteriditis together, they are not efficient for protection [31]. A main reason could be that as *Salmonella* can switch flagella production on and off, then some *Salmonella* will always escape these sIgA, and seed the infection [32]. An additional possibility could be that flagella may more easily break, especially as distance between bacteria bound by flagella (long) is likely larger than for bacteria bound by O-antigens (on chains shorter than flagellas) [33], and thus the shear forces would be larger. Further, the mechanical properties of the outer sugar layer of the gram negative bacteria could vary, and thus could be used to tune interactions. However, it would add another constraint on bacteria, and the general result that the growth rate compared to the replication rate is at least dampened by the cluster formation would remain.

In the crowded environment of the gut, it is hard for the host to identify the good and the bad bacteria. That vaccination with dead bacteria is sufficient to produce sIgA and protection, shows that the host does not discriminate well against which bacteria they produce sIgA, as these dead bacteria do not harm. Linking the effect (here the clustering) of the immune effectors with a property directly relevant to the potential bacterial pathogeneicity (here the replication rate) avoids to make complex decisions about which bacteria to produce effectors against.

Supporting information

S1 Text. Appendices and supplementary figures.
(PDF)

S1 File. Microscopy images for 3 of the mice only sampled at 4h.
(ZIP)

S2 File. Microscopy images for the other 4 mice only sampled at 4h.
(ZIP)

S3 File. Microscopy images of the mice only sampled at 5h.
(ZIP)

S4 File. Microscopy images at 4h of mice sampled sequentially.
(ZIP)

S5 File. Microscopy images at 5h of mice sampled sequentially.
(ZIP)

Acknowledgments

Author Contributions

Conceptualization: Florence Bansept, Claude Loverdo.

Investigation: Florence Bansept, Claude Loverdo.

Methodology: Florence Bansept, Claude Loverdo.

Resources: Kathrin Schumann-Moor, Médéric Diard, Wolf-Dietrich Hardt, Emma Slack.

Supervision: Claude Loverdo.

Writing – original draft: Florence Bansept, Emma Slack, Claude Loverdo.

Writing – review & editing: Florence Bansept, Kathrin Schumann-Moor, Médéric Diard, Wolf-Dietrich Hardt, Emma Slack, Claude Loverdo.

References

1. Helander HF, Fändriks L. Surface area of the digestive tract—revisited. Scandinavian journal of gastroenterology. 2014; 49(6):681–689. https://doi.org/10.3109/00365521.2014.898326 PMID: 24694282

2. Casteleyn C, Rekecki A, Van der Aa A, Simoens P, Van den Broeck W. Surface area assessment of the murine intestinal tract as a prerequisite for oral dose translation from mouse to man. Laboratory animals. 2010; 44(3):176–183. https://doi.org/10.1258/la.2009.009112 PMID: 20007641

3. Sender R, Fuchs S, Milo R. Revised estimates for the number of human and bacteria cells in the body. PLoS biology. 2016; 14(8):e1002533. https://doi.org/10.1371/journal.pbio.1002533 PMID: 27541692

4. Stecher B, Hardt WD. The role of microbiota in infectious disease. Trends in microbiology. 2008; 16(3):107–114. https://doi.org/10.1016/j.tim.2007.12.008 PMID: 18280160

5. Dishaw LJ, Cannon JP, Litman GW, Parker W. Immune-directed support of rich microbial communities in the gut has ancient roots. Developmental & Comparative Immunology. 2014; 47(1):36–51. https://doi.org/10.1016/j.dci.2014.06.011

6. Donaldson GP, Lee SM, Mazmanian SK. Gut biogeography of the bacterial microbiota. Nature Reviews Microbiology. 2016; 14(1):20. https://doi.org/10.1038/nrmicro3552 PMID: 26499895

7. Williams R, Gibbons R. Inhibition of bacterial adherence by secretory immunoglobulin A: a mechanism of antigen disposal. Science. 1972; 177(4050):697–699. https://doi.org/10.1126/science.177.4050.697 PMID: 5054144

8. Strugnell RA, Wijburg OL. The role of secretory antibodies in infection immunity. Nature Reviews Microbiology. 2010; 8(9):656. https://doi.org/10.1038/nrmicro2384 PMID: 20694027

9. Cremer J, Arnoldini M, Hwa T. Effect of water flow and chemical environment on microbiota growth and composition in the human colon. Proceedings of the National Academy of Sciences. 2017; 114 (25):6438–6443. https://doi.org/10.1073/pnas.1619598114

10. Logan SL, Thomas J, Yan J, Baker RP, Shields DS, Xavier JB, et al. The Vibrio cholerae type VI secretion system can modulate host intestinal mechanics to displace gut bacterial symbionts. Proceedings of the National Academy of Sciences. 2018; 115(16):E3779–E3787. https://doi.org/10.1073/pnas.1720133115

11. Endt K, Stecher B, Chaffron S, Slack E, Tchitchek N, Benecke A, et al. The microbiota mediates pathogen clearance from the gut lumen after non-typhoidal Salmonella diarrhea. PLoS pathogens. 2010; 6 (9):e1001097. https://doi.org/10.1371/journal.ppat.1001097 PMID: 20844578

12. Moor K, Diard M, Sellin ME, Felmy B, Wotzka SY, Toska A, et al. High-avidity IgA protects the intestine by enchaining growing bacteria. Nature. 2017; 544(7651):498–502. https://doi.org/10.1038/nature22058 PMID: 28405025

13. Kudoh K, Shimizu J, Ishiyama A, Wada M, Takita T, Kanke Y, et al. Secretion and excretion of immunoglobulin A to cecum and feces differ with type of indigestible saccharides. Journal of nutritional science and vitaminology. 1999; 45(2):173–181. https://doi.org/10.3177/jnsv.45.173 PMID: 10450558

14. Tees DF, Coenen O, Goldsmith HL. Interaction forces between red cells agglutinated by antibody. IV. Time and force dependence of break-up. Biophysical Journal. 1993; 65(3):1318–1334. https://doi.org/10.1016/S0006-3495(93)81180-9 PMID: 8241411

15. Evans EA, Calderwood DA. Forces and bond dynamics in cell adhesion. Science. 2007; 316 (5828):1148–1153. https://doi.org/10.1126/science.1137592 PMID: 17525329

16. McGrady E, Ziff RM. "Shattering" transition in fragmentation. Physical review letters. 1987; 58(9):892. https://doi.org/10.1103/PhysRevLett.58.892 PMID: 10035065

17. Odell J, Keller A. Flow-induced chain fracture of isolated linear macromolecules in solution. Journal of Polymer Science Part B: Polymer Physics. 1986; 24(9):1889–1916. https://doi.org/10.1002/polb.1986.090240901

18. Gherardi M, Amato A, Bouly JP, Cheminant S, Ferrante MI, d'Alcalá MR, et al. Regulation of chain length in two diatoms as a growth-fragmentation process. Physical Review E. 2016; 94(2):022418. https://doi.org/10.1103/PhysRevE.94.022418 PMID: 27627344

19. Brandtzaeg P. Role of secretory antibodies in the defence against infections. International Journal of Medical Microbiology. 2003; 293(1):3–15. https://doi.org/10.1078/1438-4221-00241 PMID: 12755363

20. Evans E, Berk D, Leung A. Detachment of agglutinin-bonded red blood cells. I. Forces to rupture molecular-point attachments. Biophysical Journal. 1991; 59(4):838–848. https://doi.org/10.1016/S0006-3495(91)82296-2 PMID: 2065188

21. Hulls C, Lentle RG, de Loubens C, Janssen PW, Chambers P, Stafford KJ. Spatiotemporal mapping of ex vivo motility in the caecum of the rabbit. Journal of Comparative Physiology B. 2012; 182(2):287–297. https://doi.org/10.1007/s00360-011-0610-2

22. Janssen PWM, Lentle RG, Asvarujanon P, Chambers P, Stafford KJ, Hemar Y. Characterization of flow and mixing regimes within the ileum of the brushtail possum using residence time distribution analysis with simultaneous spatio-temporal mapping. The Journal of Physiology. 2007; 582(3):1239–1248. https://doi.org/10.1113/jphysiol.2007.134403 PMID: 17495038

23. Lentle R, Janssen P. Physical characteristics of digesta and their influence on flow and mixing in the mammalian intestine: a review. Journal of Comparative Physiology B. 2008; 178(6):673–690. https://doi.org/10.1007/s00360-008-0264-x

24. Kim HJ, Huh D, Hamilton G, Ingber DE. Human gut-on-a-chip inhabited by microbial flora that experiences intestinal peristalsis-like motions and flow. Lab on a Chip. 2012; 12(12):2165. https://doi.org/10.1039/c2lc40074j PMID: 22434367

25. Lentle RG, Loubens C. A review of mixing and propulsion of chyme in the small intestine: fresh insights from new methods. Journal of Comparative Physiology B. 2015; p. 369–387. https://doi.org/10.1007/s00360-015-0889-5

26. Cremer J, Segota I, Yang Cy, Arnoldini M, Sauls JT, Zhang Z, et al. Effect of flow and peristaltic mixing on bacterial growth in a gut-like channel. Proceedings of the National Academy of Sciences. 2016; 113(41):11414–11419. https://doi.org/10.1073/pnas.1601306113

27. Wiles TJ, Jemielita M, Baker RP, Schlomann BH, Logan SL, Ganz J, et al. Host gut motility promotes competitive exclusion within a model intestinal microbiota. PLoS biology. 2016; 14(7):e1002517. https://doi.org/10.1371/journal.pbio.1002517 PMID: 27458727

28. Fournier B, Parkos C. The role of neutrophils during intestinal inflammation. Mucosal immunology. 2012; 5(4):354. https://doi.org/10.1038/mi.2012.24 PMID: 22491176

29. Mirpuri J, Raetz M, Sturge CR, Wilhelm CL, Benson A, Savani RC, et al. Proteobacteria-specific IgA regulates maturation of the intestinal microbiota. Gut microbes. 2014; 5(1):28–39. https://doi.org/10.4161/gmic.26489 PMID: 24637807

30. Richman LK, Brown WR. Immunochemical characterization of IgM in human intestinal fluids. The Journal of Immunology. 1977; 119(4):1515–1519. PMID: 894050

31. Iankov ID, Petrov DP, Mladenov IV, Haralambieva IH, Mitov IG. Lipopolysaccharide-specific but not anti-flagellar immunoglobulin A monoclonal antibodies prevent Salmonella enterica serotype Enteritidis invasion and replication within HEp-2 cell monolayers. Infection and immunity. 2002; 70(3):1615–1618. https://doi.org/10.1128/IAI.70.3.1615-1618.2002 PMID: 11854252

32. Diard M, Garcia V, Maier L, Remus-Emsermann MN, Regoes RR, Ackermann M, et al. Stabilization of cooperative virulence by the expression of an avirulent phenotype. Nature. 2013; 494(7437):353. https://doi.org/10.1038/nature11913 PMID: 23426324

33. Liu B, Knirel YA, Feng L, Perepelov AV, Senchenkova SN, Reeves PR, et al. Structural diversity in Salmonella O antigens and its genetic basis. FEMS microbiology reviews. 2014; 38(1):56–89. https://doi.org/10.1111/1574-6976.12034 PMID: 23848592